Electron spin relaxation in cubic GaN quantum dots: Perturbation theory and exact diagonalization study

M. Q. Weng,[1,2] Y. Y. Wang,[2] and M. W. Wu[1,2,*]

[1]*Hefei National Laboratory for Physical Sciences at Microscale, University of Science and Technology of China, Hefei, Anhui, 230026, China*

[2]*Department of Physics, University of Science and Technology of China, Hefei, Anhui, 230026, China*

(Received 24 September 2008; revised manuscript received 19 February 2009; published 10 April 2009)

The spin relaxation-time T_1 in zinc-blende GaN quantum dot is investigated for different magnetic field, well width, and quantum dot diameter. The spin relaxation caused by the two most important spin-relaxation mechanisms in zinc-blende semiconductor quantum dots, i.e., the electron-phonon scattering in conjunction with the Dresselhaus spin-orbit coupling and the second-order process of the hyperfine interaction combined with the electron-phonon scattering, are systematically studied. The relative importance of the two mechanisms are compared in detail under different conditions. It is found that due to the small spin-orbit coupling in GaN, the spin relaxation caused by the second-order process of the hyperfine interaction combined with the electron-phonon scattering plays much more important role than it does in the quantum dot with narrower band gap and larger spin-orbit coupling, such as GaAs and InAs.

DOI: 10.1103/PhysRevB.79.155309 PACS number(s): 73.21.La, 71.70.Ej, 85.75.−d

I. INTRODUCTION

The wide-band-gap group III nitride semiconductor GaN has emerged as a leading material for a variety of new devices,[1,2] ranging from the blue laser[3,4] to high-power electronic devices,[5] by utilizing its electronic and optical properties. Recently the magnetic properties of GaN-based nanostructures have also attracted much attention, due to the potential application in spintronic device.[6] Understanding the carrier spin-relaxation mechanism in GaN is of great importance in the design and the realization of GaN-based spin device. So far, much effort has been devoted to the experimental study of the spin relaxation in different GaN structures, including GaN epilayers,[7–10] GaN quantum wells,[11–13] and GaN quantum dots (QDs).[14] Most of these works focus on the spin lifetime in the hexagonal wurtzite GaN structures, which are easier to grow than the cubic structures. However, the spin-orbit coupling (SOC) in wurtzite GaN structure is much larger than that of cubic GaN due to the strong built-in electric field caused by the spontaneous and piezoelectric polarizations.[15,16] The electron/exciton spin lifetime of different wurtzite GaN nanostructures ranges from a few to a few hundred picoseconds while the exciton spin-relaxation time is of nanoseconds for the cubic GaN epilayer[10] and is even longer in cubic GaN QD.[14] On the theoretical side, spin-relaxation times of electron and hole in bulk cubic GaN are calculated and are found to be two or three orders of magnitude longer than those in GaAs.[17,18] However, the electron-spin properties in cubic GaN QDs are less well understood and many questions, such as what the dominant spin-relaxation mechanism is, remain open. In this paper, we will systematically study the electron-spin relaxation in cubic GaN QD under different conditions.

There are many spin-relaxation mechanisms in QDs.[19–24] In cubic semiconductor QDs, the most important two mechanisms are: (1) the electron-phonon scattering in conjunction with the SOC and (2) the second-order process of the hyperfine interaction combined with the electron-phonon scattering.[22–24] In GaAs QD, it was shown that the first mechanism is the dominant spin-relaxation mechanism for quite wide range of parameters due to the large SOC.[23] Since the SOC in GaN is much smaller than that of GaAs, which of these two mechanisms dominates spin relaxation need to be further examined.

We organize the paper as following: in Sec. II we set up the model and give the Hamiltonian. The two most important electron-spin relaxation mechanisms are discussed and the formula of the corresponding spin-relaxation rates are presented. We then calculate the spin-relaxation rates of a QD embedded in a narrow quantum well analytically using perturbation theory in Sec. III. We further present the exact spin-relaxation rates under different conditions by numerical method in Sec. IV and summarize in Sec. V.

II. MODEL AND SPIN RELAXATION RATE

We consider one-electron spin in a single GaN QD embedded in a quantum well with well width a. A magnetic field $\mathbf{B}$ is applied. The Hamiltonian of the system composed of the electron and the lattice is given by

$$H_T = H_e + H_L + H_{eL}, \tag{1}$$

where H_e, H_L, and H_{eL} are the Hamiltonians of the electron, the lattice, and their interaction, respectively. The electron Hamiltonian H_e can be written as

$$H_e = H_0 + H_{\mathrm{SO}} = \left[\frac{\mathbf{P}^2}{2m^*} + V_c(x,y) + V_z(z) + H_Z\right] + H_{\mathrm{SO}}, \tag{2}$$

where H_0 is the Hamiltonian without the SOC, m^* is the electron effective mass, and $\mathbf{P}=-i\hbar\nabla+\frac{e}{c}\mathbf{A}$ is the kinetic momentum with $\mathbf{A}=\mathbf{B}\times\mathbf{r}$. $V_z(z)$ is the quantum well confinement. In this paper, it is assumed to be a hard wall confinement with width a. $V_c(x,y)=\frac{1}{2}m^*\omega_0^2(x^2+y^2)$ is the in-plane

confinement of QD with diameter $d_0=\sqrt{\hbar\pi/m^*\omega_0}$. $H_Z=\frac{1}{2}g\mu_B\mathbf{B}\cdot\boldsymbol{\sigma}$ is the Zeeman energy with g, μ_B, and $\boldsymbol{\sigma}$ being the g factor of electron, Bohr magneton and Pauli matrix, respectively. $H_{\rm so}$ is the Hamiltonian of the SOC. In cubic GaN the dominant SOC term is Dresselhaus term,[25] which reads[26]

$$H_{\rm so}=\frac{1}{\hbar^3}\gamma_0[(P_yP_xP_y-P_zP_xP_z)\sigma_x+(P_zP_yP_z-P_xP_yP_x)\sigma_y+(P_xP_zP_x-P_yP_zP_y)\sigma_z], \tag{3}$$

with γ_0 being the Dresselhaus coefficient. The eigenwavefunction $|\ell\rangle$ and the eigenenergy $\varepsilon_\ell(\ell=1,2,\cdots)$ of H_e can be obtained from the perturbation theory or from the exact diagonalization method,[21] using the eigenstates of H_0 as basis. The Hamiltonian of the lattice is consisted of two parts: $H_L=H_{\rm ph}+H_{\rm nuclei}$. $H_{\rm ph}=\Sigma_{\mathbf{q}\eta}\hbar\omega_{\mathbf{q}\eta}a^\dagger_{\mathbf{q}\eta}a_{\mathbf{q}\eta}$ represents the Hamiltonian of the phonons with $\omega_{\mathbf{q}\eta}$ standing for the phonon energy spectrum of branch η and momentum $\mathbf{q}$ and $a^\dagger_{\mathbf{q}\eta}/a_{\mathbf{q}\eta}$ being the corresponding phonon creation/annihilation operator. $H_{\rm nuclei}=\Sigma_j\gamma_I\mathbf{B}\cdot\mathbf{I}_j$ is the Zeeman term of the lattice nuclear spins in the external magnetic field with γ_I and $\mathbf{I}_j$ denoting the gyro-magnetic ratio and spin of jth nucleus, respectively. The interaction between the electron and the lattice also has two parts: $H_{eL}=H_{\rm ep}+H_{eI}$. $H_{\rm ep}$ is the electron-phonon scattering and is given by $H_{\rm ep}=\Sigma_{\mathbf{q}\eta}M_{\mathbf{q}\eta}(a_{\mathbf{q}\eta}+a^\dagger_{-\mathbf{q}\eta})e^{i\mathbf{q}\cdot\mathbf{r}}$, where $M_{\mathbf{q}\eta}$ is the matrix element of the electron-phonon interaction. $|M_{\mathbf{q}sl}|^2=\hbar\Xi^2q/2\rho v_{sl}$ for the electron-phonon coupling due to the deformation potential. For the piezoelectric coupling, $|M_{\mathbf{q}pl}|^2=(32\hbar\pi^2e^2e_{14}^2/\kappa^2\rho v_{sl})\times[(3q_xq_yq_z)^2/q^7]$ for the longitudinal phonon mode and $\Sigma_{j=1,2}|M_{\mathbf{q}pt_j}|^2=[32\hbar\pi^2e^2e_{14}^2/(\kappa^2\rho v_{st}q^5)][q_x^2q_y^2+q_y^2q_z^2+q_z^2q_x^2-(3q_xq_yq_z)^2/q^2]$ for the two transverse modes. Here Ξ stands for the acoustic deformation potential; ρ is the GaAs volume density; e_{14} is the piezoelectric constant and κ denotes the static dielectric constant. The acoustic phonon-spectra $\omega_{\mathbf{q}l}=v_{sl}q$ for the longitudinal mode and $\omega_{\mathbf{q}t}=v_{st}q$ for the transverse modes with v_{sl} and v_{st} representing the corresponding sound velocities. H_{eI} is the electron-nucleus hyperfine interaction H_{eI}, which can be written as $H_{eI}=\Sigma_jAv_0\mathbf{S}\cdot\mathbf{I}_j\delta(\mathbf{r}-\mathbf{R}_j)$, where v_0 is the volume of the unit cell of the lattice, $\mathbf{S}$ is the spin of the electron, $\mathbf{r}$ and $\mathbf{R}_j$ are the position of the electron, and the jth nucleus, respectively. A stands for the hyperfine interaction coupling constant.

In the Hamiltonian [Eq. (1)], we only include the terms related to the two dominant spin-relaxation mechanisms. One is the electron-phonon scattering in conjunction with the Dresselhaus SOC. The SOC mixes the spin-up and spin-down states to form the majority spin-up and spin-down states. The direct coupling to the phonon causes the transition between the majority spin-up and spin-down states and results in the spin relaxation. The transfer-matrix element is $M_{\mathbf{q}\eta}$. This spin mechanism will be referred to as "Mechanism I" hereafter. The other is the second-order process of the hyperfine interaction combined with the electron-phonon interaction in which not only the SOC mixes the spin-up and spin-down states, but also the nuclei flip the electron spin. As the phonon compensates the energy difference, this mechanism also leads to spin relaxation. In the following, it is called "Mechanism II." The transfer matrix between states $|\ell_1\rangle$ and $|\ell_2\rangle$ of Mechanism II can be written as

$$V_{eI-\rm ph}=|\ell_2\rangle\left[\sum_{m\neq\ell_1}\frac{\langle\ell_2|H_{\rm ep}|m\rangle\langle m|H_{eI}|\ell_1\rangle}{\varepsilon_{\ell_1}-\varepsilon_m}+\sum_{m\neq\ell_2}\frac{\langle\ell_2|H_{eI}|m\rangle\langle m|H_{\rm ep}|\ell_1\rangle}{\varepsilon_{\ell_2}-\varepsilon_m}\right]\langle\ell_1|=\sum_{\mathbf{q}\eta}\mathcal{M}_{\mathbf{q}\eta}(a_{\mathbf{q}\eta}+a^\dagger_{-\mathbf{q}\eta}), \tag{4}$$

with

$$\mathcal{M}_{\mathbf{q}\eta}=|\ell_2\rangle\left[\sum_{m\neq\ell_1}\frac{\langle\ell_2|M_{\mathbf{q}\eta}e^{i\mathbf{q}\cdot\mathbf{r}}|m\rangle\langle m|H_{eI}|\ell_1\rangle}{\varepsilon_{\ell_1}-\varepsilon_m}+\sum_{m\neq\ell_2}\frac{\langle\ell_2|H_{eI}|m\rangle\langle m|M_{\mathbf{q}\eta}e^{i\mathbf{q}\cdot\mathbf{r}}|\ell_1\rangle}{\varepsilon_{\ell_2}-\varepsilon_m}\right]\langle\ell_1|, \tag{5}$$

where the summation of $|m\rangle$ runs over all possible intermediate states.

To calculate the spin-relaxation time, one can use the perturbative approach based on the calculation of the transition rates from Fermi's golden rule.[19–21,24,27] Nonperturbative calculation using equation of motion method has also been proposed to study the spin relaxation of the system with large SOC at high-temperature regime.[23,24] For the system with weak SOC at low-temperature regime, these two approaches produce the same results. In the cubic GaN QD, since the SOC is pretty weak,[28] the perturbative approach gives sufficient accurate spin-relaxation rate and is therefore adopted in the present work.

Using the Fermi's golden rule, one can obtain the spin-relaxation rate as[23]

$$T_1^{-1}=\sum_{if}(f_{i+}\Gamma_{i+\to f-}+f_{i-}\Gamma_{i-\to f+}). \tag{6}$$

Here $f_{i\pm}$ is the Maxwell distribution since we study the spin relaxation of single electron confined in the QD. "+/−" stand for the states with the majority up/down-spin. The scattering rate $\Gamma_{i\to f}$ reads

$$\Gamma_{i\to f}=\frac{2\pi}{\hbar}\sum_{\mathbf{q}\eta}|\langle f|\mathcal{X}_{\mathbf{q}\eta}|i\rangle|^2[n_{\mathbf{q}\eta}\delta(\varepsilon_f-\varepsilon_i-\hbar\omega_{\mathbf{q}\eta})+(n_{\mathbf{q}\eta}+1)\delta(\varepsilon_f-\varepsilon_i+\hbar\omega_{\mathbf{q}\eta})], \tag{7}$$

where $\mathcal{X}_{\mathbf{q}\eta}=M_{\mathbf{q}\eta}e^{i\mathbf{q}\cdot\mathbf{r}}$ and $\mathcal{X}_{\mathbf{q}\eta}=\mathcal{M}_{\mathbf{q}\eta}$ for Mechanisms I and II, respectively. $n_{\mathbf{q}\eta}$ is the Bose distribution function for phonons.

III. ANALYTICAL RESULTS

Before presenting the full exact diagonalization result, let us first look at the analytical result of the spin-relaxation rate of a QD embedded in a narrow quantum well by perturbatively solving the electron Hamiltonian [Eq. (2)] to the second order of the SOC.

Due to the symmetry of the QD in the x-y plane, $\mathbf{B}$ can be assumed to be $(B_\parallel,0,B_\perp)$ with $B_\parallel=B\sin\theta$ and $B_\perp=B\cos\theta$

being the components along the x axis and z axis, and θ representing the angle between the magnetic field direction and the z axis. The eigenstate of the electron Hamiltonian without the SOC (H_0) $|n_z n l \sigma\rangle$ is characterized by the quantum number of quantum well confinement, radial, angular, and spin freedoms $n_z(=1,2,\cdots)$, $n(=0,1,\cdots)$, $l(=0,\pm 1,\cdots)$, and $\sigma(=\pm 1)$, respectively, whose energy is $E_{n_z n l\sigma}=\frac{n_z^2\hbar^2\pi^2}{2m^*a^2}+(2n+|l|+1)\hbar\Omega+l\hbar\omega_{B_\perp}+\sigma E_B$, with $\Omega=\sqrt{\omega_0^2+\omega_{B_\perp}^2}$, $\omega_B=eB_\perp/(2m^*)$, and $E_B=\frac{1}{2}g\mu_B B$. In the narrow quantum well ($d_0 \gg a$), the distance of different n_z states is so large that only the lowest n_z state is relevant. Under this approximation, the spin-orbit coupling can be expressed as $H_{\rm so}=\frac{1}{\hbar}\gamma_0(\pi/a)^2(-P_x\sigma_x+P_y\sigma_y)$. Up to the first-order perturbation, the lowest two eigenstates of the electron with the SOC are

$$|\ell_1\rangle = |001\rangle + \mathcal{B}^{1,+}_{011,001}|011\rangle - \mathcal{B}^{3,+}_{01-1,001}|01-1\rangle + \mathcal{B}^{1,-}_{0-11,001}|0-11\rangle + \mathcal{B}^{2,-}_{0-1-1,001}|0-1-1\rangle,$$

$$|\ell_2\rangle = |00-1\rangle + \mathcal{B}^{2,+}_{011,00-1}|011\rangle - \mathcal{B}^{1,+}_{01-1,00-1}|01-1\rangle - \mathcal{B}^{3,-}_{0-11,00-1}|0-11\rangle - \mathcal{B}^{1,-}_{0-1-1,00-1}|0-1-1\rangle, \quad (8)$$

where $\mathcal{B}^{1,\pm}_{nl\sigma,n'l'\sigma'}=i\frac{1}{2}\hbar\gamma_c\alpha(1\pm\omega_{B_\perp}/\Omega)\sin\theta/(E_{nl\sigma}-E_{n'l'\sigma'})$, $\mathcal{B}^{2,\pm}_{nl\sigma,n'l'\sigma'}=i\frac{1}{2}\hbar\gamma_c\alpha(1\pm\omega_{B_\perp}/\Omega)(1+\cos\theta)/(E_{nl\sigma}-E_{n'l'\sigma'})$, and $\mathcal{B}^{3,\pm}_{nl\sigma,n'l'\sigma'}=i\frac{1}{2}\hbar\gamma_c\alpha(1\pm\omega_{B_\perp}/\Omega)(1-\cos\theta)/(E_{nl\sigma}-E_{n'l'\sigma'})$. The corresponding eigenenergies of these states read

$$\varepsilon_1 = E_{001} + |\mathcal{B}^{1,+}_{011,001}|^2(E_{011}-E_{001}) - |\mathcal{B}^{3,+}_{01-1,001}|^2(E_{01-1}-E_{001}) + |\mathcal{B}^{1,-}_{0-11,001}|^2(E_{0-11}-E_{001}) + |\mathcal{B}^{2,-}_{0-1-1,001}|^2(E_{0-1-1}-E_{001}),$$

$$\varepsilon_2 = E_{00-1} + |\mathcal{B}^{2,+}_{011,00-1}|^2(E_{011}-E_{00-1}) - |\mathcal{B}^{1,+}_{01-1,00-1}|^2(E_{01-1}-E_{00-1}) - |\mathcal{B}^{3,-}_{0-11,00-1}|^2(E_{0-11}-E_{00-1}) - |\mathcal{B}^{1,-}_{0-1-1,00-1}|^2(E_{0-1-1}-E_{00-1}). \quad (9)$$

It is noted that in the above equations, we have included the second-order correction of the SOC on the energy, which is crucial to the study of the spin relaxation using perturbation method as pointed out by Cheng *et al.*[21] It is also noted that the state index n_z is dropped in the above equations since it is always 1 in the narrow quantum well approximation. $|\ell_1\rangle$ and $|\ell_2\rangle$ are the lowest majority spin-up and spin-down states, respectively. At the low-temperature regime, the electron mainly distributes on these two states. Therefore, T_1 basically equals the spin-relaxation time between these two states. It is further noted that at low-temperature regime, the main electron-phonon scattering comes from the electron coupling to the transverse phonon via piezoelectric field. With these approximations, the spin-relaxation rate due to Mechanism I is given by

$$\Gamma_1 = c(2n_{\mathbf{q}}+1)\alpha q\int_0^{\pi/2} d\theta'\,\sin^3\theta'(\sin^4\theta'+8\cos^4\theta') \times e^{-q^2\sin^2\theta'/2} I^2\left(\frac{1}{2}qa\alpha\cos\theta'\right) \times\left[2\mathcal{P}_1^2+(\mathcal{P}_2^2+\mathcal{P}_3^2-2\mathcal{P}_1^2)\frac{1}{4}q^2\sin^2\theta' + (\mathcal{P}_4^2+\mathcal{P}_5^2+2\mathcal{P}_1^2)\frac{1}{16}q^4\sin^4\theta'\right], \quad (10)$$

where $c=\pi e^2 e_{14}^2/(\hbar D v_{st}^2\kappa^2)$, $q=\Delta E/(\hbar v_{st}\alpha)$ with $\Delta E=|\varepsilon_2-\varepsilon_1|$, and $\alpha=\sqrt{m^*\Omega/\hbar}$. $I(x)=\pi^2\sin(x)/[x(\pi-x)(\pi+x)]$ denotes the form factor along z direction due to the quantum well confinement. In the above equation, $\mathcal{P}_1=\mathcal{A}_1+\mathcal{A}_2-\mathcal{A}_3-\mathcal{A}_4$ with $\mathcal{A}_1=|\mathcal{B}^{1,+}_{011,001}\mathcal{B}^{2,+}_{011,00-1}|$, $\mathcal{A}_2=|\mathcal{B}^{3,+}_{01-1,001}\mathcal{B}^{1,+}_{01-1,00-1}|$, $\mathcal{A}_3=|\mathcal{B}^{1,-}_{0-11,001}\mathcal{B}^{3,-}_{0-11,00-1}|$, and $\mathcal{A}_4=|\mathcal{B}^{2,-}_{0-1-1,001}\mathcal{B}^{1,-}_{0-1-1,00-1}|$; $\mathcal{P}_2=-|\mathcal{B}^{2,+}_{011,00-1}|+|\mathcal{B}^{3,-}_{0-11,00-1}|-|\mathcal{B}^{3,+}_{01-1,001}|+|\mathcal{B}^{2,-}_{0-1-1,001}|$; $\mathcal{P}_3=-|\mathcal{B}^{2,+}_{011,00-1}|-|\mathcal{B}^{3,-}_{0-11,00-1}|+|\mathcal{B}^{3,+}_{01-1,001}|+|\mathcal{B}^{2,-}_{0-1-1,001}|$, $\mathcal{P}_4=\mathcal{C}_1-\mathcal{C}_2+\mathcal{C}_3-\mathcal{C}_4$, $\mathcal{P}_5=\mathcal{C}_1-\mathcal{C}_2-\mathcal{C}_3+\mathcal{C}_4$ with $\mathcal{C}_1=|\mathcal{B}^{1,-}_{011,001}\mathcal{B}^{3,+}_{0-11,00-1}|$, $\mathcal{C}_2=|\mathcal{B}^{1,-}_{01-1,001}\mathcal{B}^{3,+}_{0-1-1,00-1}|$, $\mathcal{C}_3=|\mathcal{B}^{1,-}_{0-11,001}\mathcal{B}^{2,+}_{011,00-1}|$, and $\mathcal{C}_4=|\mathcal{B}^{1,-}_{0-1-1,001}\mathcal{B}^{2,+}_{01-1,00-1}|$. Using the material parameters of GaN QD and in consideration of the relative small magnetic field, one can write down the spin-relaxation rate due to this mechanism at zero temperature for relative small dot,

$$\Gamma_1 \propto a^{-4}d_0^8 B^5(1+\cos^2\theta), \quad (11)$$

which indicates that for fixed magnetic field magnitude, the spin relaxation under the perpendicular magnetic field is two times of that under the parallel magnetic filed. It should be noted that for $\theta=0$ case (the magnetic field is along the z axis), to the leading term, the magnetic field dependence of Γ_1 obtained here is in accordance with that obtained in Refs. 19 and 20. By assuming that the nuclei spins are independent to each other and are in equilibrium state, the spin relaxation between $|\ell_1\rangle$ and $|\ell_2\rangle$ induced by Mechanism II, with the mediation of the lowest available state, can be written as

$$\Gamma_2 = \left(\frac{A}{\varepsilon_2-\varepsilon_3}\right)^2 I(I+1)v_0\alpha^3 a^{-1}c(2n_{\mathbf{q}}+1)q^3 \times\int_0^{\pi/2} d\theta'\,\sin^5\theta'(\sin^4\theta'+8\cos^4\theta') \times e^{-q^2\sin^2\theta'/2} I^2\left(\frac{1}{2}qa\alpha\cos\theta'\right), \quad (12)$$

which at zero temperature gives

$$\Gamma_2 \propto c_3 a^{-1}d_0^4 B^3. \quad (13)$$

The ratio of the spin relaxations due to these two mechanisms is therefore

$$\Gamma_1/\Gamma_2 \propto a^{-3}d_0^4 B^2, \quad (14)$$

which gives a guideline to determine which mechanism is more important at different conditions. It is therefore expected that Mechanism II is more important for smaller QD embedded in the wider quantum well under weaker magnetic field.

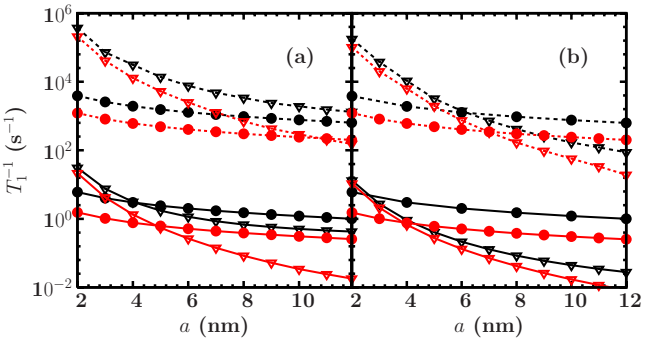

FIG. 1. (Color online) Spin relaxation rate vs the well width a in the presence of (a) perpendicular and (b) parallel magnetic fields with $B=0.5$ T (solid curves) and $B=5$ T (dotted curves). In the calculation, $d_0=10$ nm. Black (dark) curves—exact diagonalization results; red (light) curves—perturbation results. Curves with $\nabla-T_1^{-1}$ induced by the electron-phonon scattering in conjunction with the SOC; Curves with $\bullet-T_1^{-1}$ induced by the second-order process of the hyperfine interaction combined with the electron-phonon scattering.

IV. NUMERICAL RESULTS

The perturbation method gives qualitative results for us to understand the overall behavior of spin relaxation in GaN under different conditions. However, in the perturbation calculation, states with higher energy are dropped to get a manageable analytical result. It should be noted that, for the spin relaxation caused by Mechanism II, the contributions of higher intermediate states and the lowest one are of the same order with regard to hyperfine-interaction strength. Moreover, for QD embedded in wider quantum wells, contribution of the higher n_z states to the spin-orbit coupling cannot be neglected. It is expected that for $d_0 \leq a$, the spin relaxation due to Mechanism I can be different from the perturbative results. It is therefore necessary to check the accuracy of the perturbative calculation by comparing to the exact diagonalization with sufficient basis functions included.

In Fig. 1, we present the spin-relaxation rates as functions of well width in GaN QD under different conditions obtained by the exact diagonalization and perturbation. The material parameters of GaN are listed in Table I.[29–32] The Dresselhaus coefficient γ_0 is chosen to be 0.51 Å$^3\cdot$eV according to the latest calculation.[28] It is seen that the perturbation results describe the qualitative behavior of the spin relaxation pretty well. For the cases we study here, the spin relaxation caused by the electron-phonon scattering in conjunction with the SOC from the perturbation is very close to the exact diagonalization result in narrow quantum well. When the well width becomes larger, the difference between perturbative and exact diagonalization result also grows as contribution of the higher n_z states becomes more and more important. On the other hand, for the spin relaxation caused by the hyperfine interaction together with electron-phonon interaction, the difference between perturbative and exact diagonalization results almost does not change with the well width. For this mechanism, the relaxation rate from exact diagonalization method is always about one order of magnitude higher than that obtained from the perturbation calculation for the cases we study. This indicates the contribution of the higher states are important to the quantitative calculation of the spin relaxation. In the following, we only present the results of exact diagonalization unless otherwise specified. We now focus on how the spin relaxation induced by the two mechanisms change with a. It is seen that the spin relaxations induced by the two mechanisms both decrease with a. The spin relaxation due to Mechanism I decreases much faster than that due to Mechanism II. As a result, Mechanism II becomes more and more important when the quantum well width increases. This can be understood from the perturbation result. As one can see from Eqs. (11) and (13) that the relaxation rate Γ_1 decreases with a as a^{-4}, while Γ_2 is proportional to a^{-1}. We then pay attention to the relative importance of these two mechanisms. For the vertical-magnetic-field case in Fig. 1(a), for $B=5$ T, spin relaxation due to Mechanism I is always the dominant spin-relaxation mechanism. When B decreases to 0.5 T, Mechanism II almost dominates the spin relaxation except at very small well width ($a<4$ nm). For the parallel-magnetic-field case in Fig. 1(b), Mechanism II is even more important and dominates the spin relaxation for $a>6$ nm and >2.5 nm when $B=5$ T and 0.5 T, respectively. This is quite different from the cubic materials with narrower band gap and larger SOC such as GaAs, in which the spin relaxation due to Mechanism I is usually 2–3 orders of magnitude stronger than that due to Mechanism II. But thanks to the small SOC, the spin relaxation caused by the nuclei plays a much more important role in GaN QD. It is also worth noting that the hyperfine interaction and the SOC can also cause spin dephasing. Previous studies on GaAs QD have shown that the hyperfine interaction usually dominates the spin dephasing at low temperature.[23,33] It is expected that the spin dephasing in GaN QD is also dominated by the hyperfine interaction due to the very small SOC in this material. Our numerical results using the approach in Ref. 23 show that this is indeed true, e.g., for QD of $a=5$ nm and $d_0=10$ nm, T_2 induced by the hyperfine interaction is about 5 orders of magnitude shorter than that induced by the SOC under parallel magnetic field of 0.5 T when $T=0$ K. As we are interested in the difference between GaN and GaAs QDs, we will not further address the spin dephasing in the paper.

In Fig. 2 the QD diameter dependence of the spin relaxation is presented under the magnetic field (a) perpendicular and (b) parallel to the well plane. Both relaxation rates increase with the increase in dot size but with different speeds: $\Gamma_1 \propto d_0^8$ and $\Gamma_2 \propto d_0^4$. As a result, Mechanism I becomes more important as the size of QD grows. One can see from Fig. 2 that, under the low magnetic field ($B=0.5$ T) we show here, Mechanism II plays a very important role, or even dominates the spin relaxation for all QD whose diameter is smaller than 11 nm.

TABLE I. Parameters used in the calculation.

ρ	6.095×10^3 kg/m^3	κ	8.5
v_{st}	2.68×10^3 m/s	g	2.06
v_{sl}	6.56×10^3 m/s	Ξ	8.3 eV
e_{14}	4.3×10^9 V/m	m^*	$0.15m_0$
A	45 μeV	I	$\frac{3}{2}$

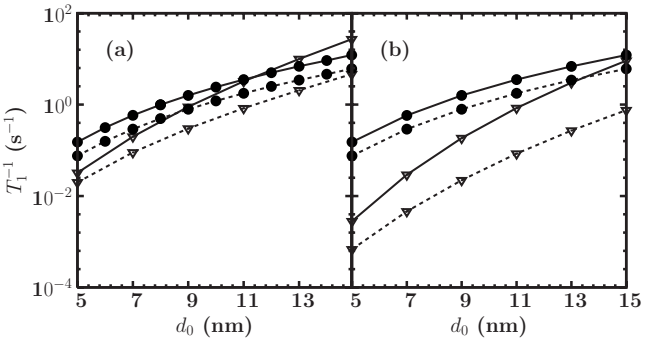

FIG. 2. Spin relaxation vs the QD diameter d_0 in the presence of (a) perpendicular and (b) parallel magnetic fields at two well widths: $a=5$ nm (solid curves) and $a=10$ nm (dotted curves). In the calculation, $B=0.5$ T. Curves with ∇–T_1^{-1} induced by the electron-phonon scattering in conjunction with the SOC; Curves with ●–T_1^{-1} induced by the second-order process of the hyperfine interaction combined with the electron-phonon scattering.

In Figs. 3(a) and 3(b) the spin relaxation rates induced by the two mechanisms are plotted as functions of the perpendicular and parallel magnetic fields, respectively. In each figure, the results are shown for both narrow well ($a=5$ nm) and relatively wide well ($a=10$ nm). It is noticed that the effect of each mechanism increases with the magnetic field as predicated by Eqs. (11) and (13). Then we pay attention to the relative importance of the two mechanisms. When the magnetic field is along the z direction, it is seen from Fig. 3 that Mechanism I is dominant when large vertical magnetic ($B>0.5$ T) is applied. However, when the magnetic is along x axis, for small well width ($a=5$ nm), Mechanism I is dominant for large magnetic field. For wider quantum well ($a=10$ nm), Mechanism II dominates the spin relaxation when $B<2.5$ T and is comparable to Mechanism I for larger magnetic field.

We then turn to study how the direction of the applied magnetic field changes the spin relaxation. In Fig. 4, we show the spin-relaxation rates as functions of the angle θ between **B** and the z axis for a fixed magnetic field amplitude. It is seen that these two mechanisms depend on the direction of the magnetic field quite differently. The spin relaxation induced by Mechanism I has a maximum when the magnetic field is along the z direction. With the increase in θ, it decreases gradually and reaches the minimum when **B** is in the x-y plane. On the other hand, the spin relaxation induced by Mechanism II almost keeps unchanged with θ. This can be understood from the perturbation result. As we can see from Eqs. (11) and (13) that the relaxation rate Γ_1 contains the term of $(1+\cos^2\theta)$, which has the largest value for $\theta=0$ and the smallest value for $\theta=\pi/2$ for the condition we considered, while Γ_2 is almost independent of θ. Overall, the changes in the spin-relaxation rates in GaN QD are mild when the direction of the magnetic field changes for both mechanisms. This is quite different from that in GaAs QD, where the spin relaxation induced by Mechanism I with the perpendicular magnetic field can be several orders of magnitude larger than that with the parallel magnetic field.[23,34] This is because in GaAs material, the SOC is usually comparable or even larger than Zeeman splitting and therefore the magnetic field direction changes the eigenenergy remarkably. Consequently, the difference between the maximum and the minimum of the spin-relaxation rates induced by Mechanism I can be several orders of magnitude different when the direction of the magnetic field changes. However, due to the small SOC in GaN, the energy difference between the lowest two eigenstates is determined by the Zeeman splitting and therefore the change in spin relaxation with the magnetic field direction is much milder.

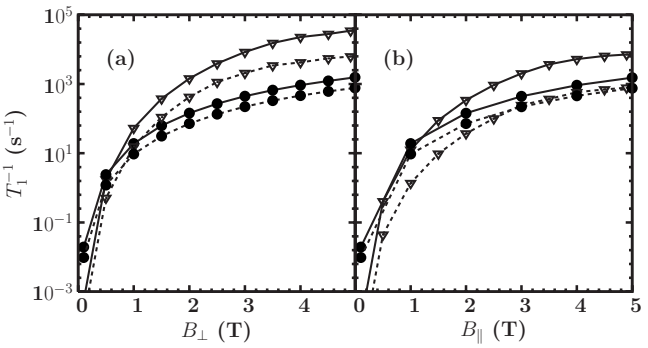

FIG. 3. Spin relaxation vs (a) perpendicular and (b) parallel magnetic field at two well widths: $a=5$ nm (solid curves) and $a=10$ nm (dotted curves). In the calculation, $d_0=10$ nm. Curves with ∇–T_1^{-1} induced by the electron-phonon scattering in conjunction with the SOC; curves with ●–T_1^{-1} induced by the second-order process of the hyperfine interaction combined with the electron-phonon scattering.

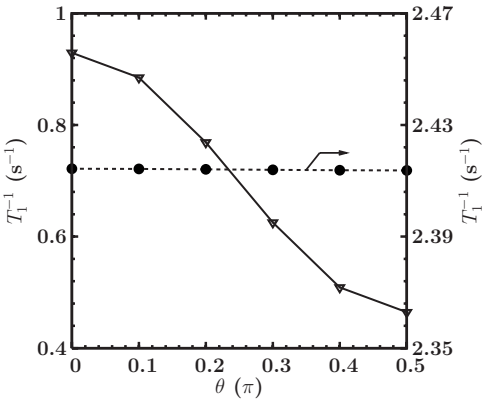

FIG. 4. Spin relaxations vs θ. In the calculation, $a=5$ nm, $B=0.5$ T, and $d_0=10$ nm. Curve with ∇–T_1^{-1} induced by the electron-phonon scattering in conjunction with the SOC; curve with ●–T_1^{-1} induced by the second-order process of the hyperfine interaction combined with the electron-phonon scattering. Note the scale of the spin relaxation induced by the second mechanism is at the right-hand side of the frame.

We further investigate how the spin-relaxation changes with the temperature. The results are shown in Fig. 5. One can see that spin relaxations induced by the two mechanisms both increase with the temperature. For low-temperature regime, the relative importance of each mechanism remains unchanged. That is, Mechanism I is more important when the magnetic field is perpendicular to the well, while Mechanism II usually plays more important role for the parallel magnetic field. Both are approximately proportional to $[2n_{\mathbf{q}}(T)+1]$

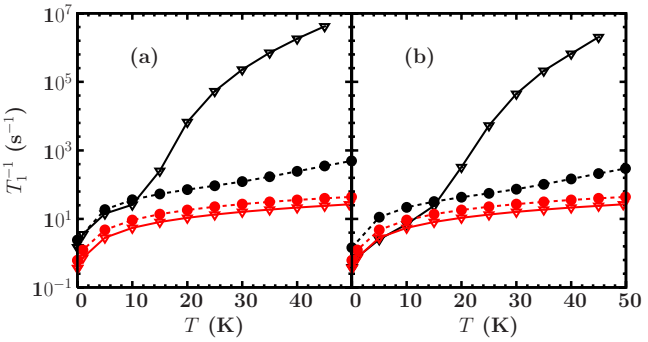

FIG. 5. (Color online) Spin relaxation vs temperature T in the presence of (a) perpendicular and (b) parallel magnetic fields. In the calculation, $a=5$ nm, $d_0=10$ nm, and $B=0.5$ T. Black (dark) curves—exact diagonalization results; red (light) curves—perturbation results. Curves with $\nabla - T_1^{-1}$ induced by the electron-phonon scattering in conjunction with the SOC; curves with ● $-T_1^{-1}$ induced by the second-order process of the hyperfine interaction combined with the electron-phonon scattering.

which is consistent with the perturbative results, i.e., Eqs. (10) and (13). However, when the temperature rises high enough ($T>10$ K), the spin relaxation induced by Mechanism I increases much quicker than Mechanism II. For both parallel and perpendicular magnetic fields, Mechanism II dominates the spin relaxation for low temperature while Mechanism I has larger contribution for high temperature. In order to understand the different temperature dependences of relaxations, we also show the spin-relaxation rates from perturbation calculation in the same figure. It is seen that the perturbation result and the exact diagonalization result of the spin relaxation due to Mechanism II agree with each other qualitatively in the temperature regime we study. However, the spin relaxation of exact diagonalization due to Mechanism I departs from the perturbation prediction in the high-temperature regime. This indicates that the perturbation method is no longer reliable for Mechanism I and should not be used to obtain the spin-relaxation rate under high temperature. This is understandable, because at low-temperature regime, the electron distribution at the high levels is negligible and only the lowest two Zeeman splitting levels are involved due to the small SOC. Therefore perturbative method is accurate enough to study the spin relaxation caused by Mechanism I. With the increase in temperature, electron can occupy higher energy levels with larger SOC. As a result, the perturbation method is no longer adequate to study the transition rates induced by Mechanism I.

V. CONCLUSION

In conclusion, we have investigated the spin relaxation-time T_1 in cubic GaN QD under different conditions by the perturbation and exact diagonalization approaches. Two leading spin-relaxation mechanisms, i.e., the electron-phonon scattering in conjunction with the SOC and the second-order process of the hyperfine interaction combined with the electron-phonon scattering, are considered. We systematically study how the spin relaxations induced by the two mechanisms change with the well width a, magnetic field B, and quantum dot diameter d_0, and demonstrate how they are different from the counter parts in GaAs/InAs quantum dots. Our results show that, the ratio of these two spin-relaxation rates is proportional to $a^{-3}B^2d_0^4$ in the low-temperature regime when the quantum well constraint is strong enough. Comparing to GaAs and InAs, the spin relaxation caused by the second-order process of the hyperfine interaction combined with the electron-phonon scattering plays much more important role in GaN material due to the small SOC. Only when the well width a is small enough and/or the magnetic field B and QD diameter d_0 are large enough, the electron-phonon scattering in conjunction with the SOC may dominate. Furthermore, how the direction of the applied magnetic field changes the spin relaxation are investigated. The spin relaxation induced by the electron-phonon scattering in conjunction with the SOC has a maximum when the magnetic field is along the z direction and reaches the minimum when the magnetic field is in the x-y plane. Nevertheless, the spin relaxation induced by the second-order process of the hyperfine interaction combined with the electron-phonon scattering keeps almost unchanged with the magnetic field direction. We also discuss the temperature dependence of the spin relaxation due to the two mechanisms. At high temperatures, the spin relaxation induced by the electron-phonon scattering in conjunction with the SOC is always dominant.

ACKNOWLEDGMENTS

This work was supported by the Natural Science Foundation of China under Grants No. 10725417 and No. 10804103, the National Basic Research Program of China under Grant No. 2006CB922005, and the Innovation Project of Chinese Academy of Sciences. One of the authors (M.W.W.) would like to thank X. Marie for valuable discussions.

*Author to whom correspondence should be addressed; mwwu@ustc.edu.cn.

[1] B. Gil, O. Briot, and R. L. Aulombard, Phys. Rev. B **52**, R17028 (1995).
[2] N. Grandjean and M. Ilegems, Proc. IEEE **95**, 1853 (2007).
[3] S. Nakamura, T. Mukai, and M. Senoh, Jpn. J. Appl. Phys., Part 2 **30**, L1998 (1991).
[4] S. Nakamura, M. Senoh, S. Nagahama, N. Iwasa, T. Yamada, T. Matsushita, H. Kiyoku, and Y. Sugimoto, Jpn. J. Appl. Phys., Part 2 **35**, L74 (1996).
[5] H. Morkoc, *Nitride Semiconductors and Devices* (Springer, New York, 1999).
[6] S. J. Pearton, C. R. Abernathy, G. T. Thaler, R. M. Frazier, D. P. Norton, F. Ren, Y. D. Park, J. M. Zavada, I. A. Buyanova, W. M.

Chen, and A. F. Hebard, J. Phys.: Condens. Matter **16**, R209 (2004).
[7] B. Beschoten, E. Johnston-Halperin, D. K. Young, M. Poggio, J. E. Grimaldi, S. Keller, S. P. DenBaars, U. K. Mishra, E. L. Hu, and D. D. Awschalom, Phys. Rev. B **63**, 121202(R) (2001).
[8] T. Kuroda, T. Yabushita, T. Kosuge, A. Tackeuchi, K. Taniguchi, T. Chinone, and N. Horio, Appl. Phys. Lett. **85**, 3116 (2004).
[9] T. Ishiguro, Y. Toda, and S. Adachi, Appl. Phys. Lett. **90**, 011904 (2007).
[10] A. Tackeuchi, H. Otake, Y. Ogawa, T. Ushiyama, and T. Fujita, Appl. Phys. Lett. **88**, 162114 (2006).
[11] S. Nagahara, M. Arita, and Y. Arakawa, Appl. Phys. Lett. **86**, 242103 (2005).
[12] S. Nagahara, M. Arita, and Y. Arakawa, Appl. Phys. Lett. **88**, 083101 (2006).
[13] W. M. Chen, I. A. Buyanova, K. Nishibayashi, K. Kayanuma, K. Seo, A. Murayama, Y. Oka, G. Thaler, R. Frazier, C. R. Abernathy, F. Ren, S. J. Pearton, C.-C. Pan, G.-T. Chen, and J.-I. Chyi, Appl. Phys. Lett. **87**, 192107 (2005).
[14] D. Lagarde, A. Balocchi, H. Carrére, P. Renucci, T. Amand, X. Marie, S. Founta and H. Mariette, Phys. Rev. B **77**, 041304(R) (2008).
[15] V. A. Fonoberov and A. A. Balandin, J. Appl. Phys. **94**, 7178 (2003).
[16] M. Julier, A. Vinattieri, M. Colocci, P. Lefebvre, B. Gil, D. Scalbert, C. A. Tran, R. F. Karlicek, Jr., and J.-P. Lascaray, Phys. Status Solidi B **216**, 341 (1999)
[17] S. Krishnamurthy, M. van Schilfgaarde, and N. Newman, Appl. Phys. Lett. **83**, 1761 (2003).
[18] Z. G. Yu, S. Krishnamurthy, M. van Schilfgaarde, and N. Newman, Phys. Rev. B **71**, 245312 (2005).
[19] A. V. Khaetskii and Y. V. Nazarov, Phys. Rev. B **64**, 125316 (2001).
[20] L. M. Woods, T. L. Reinecke, and Y. Lyanda-Geller, Phys. Rev. B **66**, 161318(R) (2002).
[21] J. L. Cheng, M. W. Wu, and C. Lü, Phys. Rev. B **69**, 115318 (2004); C. Lü, J. L. Cheng, and M. W. Wu, *ibid.* **71**, 075308 (2005).
[22] S. I. Erlingsson and Y. V. Nazarov, Phys. Rev. B **66**, 155327 (2002).
[23] J. H. Jiang, Y. Y. Wang, and M. W. Wu, Phys. Rev. B **77**, 035323 (2008).
[24] J. Voss and D. Pfannkuche, arXiv:0712.2376.
[25] G. Dresselhaus, Phys. Rev. **100**, 580 (1955).
[26] E. I. Rashba, Physica E **20**, 189 (2004).
[27] V. N. Golovach, A. Khaetskii, and D. Loss, Phys. Rev. B **77**, 045328 (2008).
[28] J. Y. Fu and M. W. Wu, J. Appl. Phys. **104**, 093712 (2008).
[29] *Numerical Data and Functional Relationships in Science and Technology*, Landolt-Börnstein, New Series, Group III, Vol. 17, Pt. A, edited by O. Madelung, M. Schultz, and H. Weiss (Springer-Verlag, Berlin, 1982.).
[30] I. Vurgaftman and J. R. Meyer, J. Appl. Phys. **94**, 3675 (2003).
[31] J. D. Albrecht, R. P. Wang, P. P. Ruden, M. Farahmand, and K. F. Brennan, J. Appl. Phys. **83**, 4777 (1998).
[32] B. Krummheuer, V. M. Axt, T. Kuhn, I. D'Amico, and F. Rossi, Phys. Rev. B **71**, 235329 (2005).
[33] A. C. Johnson, J. R. Petta, J. M. Taylor, A. Yakoby, M. D. Lukin, C. M. Marcus, M. P. Hanson, and A. C. Gossard, Nature (London) **435**, 925 (2005); F. H. L. Koppens, J. A. Folk, J. M. Elzerman, R. Hanson, L. H. W. van Beveren, I. T. Vink, H. P. Tranitz, W. Wegscheider, L. P. Kouwenhoven, and L. M. K. Vandersypen, Science **309**, 1346 (2005); S. I. Erlingsson and Y. V. Nazarov, Phys. Rev. B **70**, 205327 (2004); S. I. Erlingsson, O. N. Jouravlev, and Y. V. Nazarov, *ibid.* **72**, 033301 (2005); W. A. Coish and D. Loss, *ibid.* **72**, 125337 (2005).
[34] C. F. Destefani and S. E. Ulloa, Phys. Rev. B **72**, 115326 (2005).